

# Chasing Similarity: Distribution-aware Aggregation Scheduling (Extended Version)

Feilong Liu<sup>1</sup>, Ario Salmasi<sup>1</sup>, Spyros Blanas<sup>1</sup>, Anastasios Sidiropoulos<sup>2</sup>

<sup>1</sup>The Ohio State University, <sup>2</sup>University of Illinois at Chicago

{liu.3222,salmasi.1,blanas.2}@osu.edu, sidiropo@gmail.com

## ABSTRACT

Parallel aggregation is a ubiquitous operation in data analytics that is expressed as `GROUP BY` in SQL, `reduce` in Hadoop, or `segment` in TensorFlow. Parallel aggregation starts with an optional local pre-aggregation step and then repartitions the intermediate result across the network. While local pre-aggregation works well for low-cardinality aggregations, the network communication cost remains significant for high-cardinality aggregations even after local pre-aggregation. The problem is that the repartition-based algorithm for high-cardinality aggregation does not fully utilize the network.

In this work, we first formulate a mathematical model that captures the performance of parallel aggregation. We prove that finding optimal aggregation plans from a known data distribution is NP-hard, assuming the Small Set Expression conjecture. We propose GRASP, a GReedy Aggregation Scheduling Protocol that decomposes parallel aggregation into phases. GRASP is distribution-aware as it aggregates the most similar partitions in each phase to reduce the transmitted data size in subsequent phases. In addition, GRASP takes the available network bandwidth into account when scheduling aggregations in each phase to maximize network utilization. The experimental evaluation on real data shows that GRASP outperforms repartition-based aggregation by 3.5 $\times$  and LOOM by 2.0 $\times$ .

## 1. INTRODUCTION

Aggregation is widely used in data analytics. Parallel aggregation is executed in two steps. The first step is an optional local aggregation where data is aggregated locally, followed by a second step where data is repartitioned and transferred to the final destination node for aggregation [46, 15]. The local aggregation can reduce the amount of data transferred in the second step for algebraic aggregations, as tuples with the same GROUP BY key are aggregated to a single tuple during local aggregation [6, 53, 22, 35, 49]. Local aggregation works effectively for low-cardinality domains, such as `age`, `sex` or `country`, where data can be reduced substantially and make the cost of the repartition step negligible. However, high-cardinality aggregations see little or no benefit from local aggregation. Optimizing the repartitioning step for high-cardinality aggregation has received less research attention.

High-cardinality aggregations are surprisingly common in practice. One example is sessionization, where events in a timestamp-ordered log need to be grouped into user sessions for analysis. An exemplar is the publicly-available Yelp dataset where 5.2M reviews are aggregated into 1.3M

user sessions [54]. Even when there are no high-cardinality attributes, aggregation on composite keys of multiple attributes can lead to high-cardinality aggregations, which is common in data cube calculations [16].

This paper focuses on reducing the communication cost for high-cardinality aggregations. We classify aggregations into two types: the all-to-one aggregation and the all-to-all aggregation. In all-to-one aggregation, one coordinator collects and aggregates data from all compute nodes as in Redshift [40] and Citus [7]. All-to-one aggregation frequently happens as the last stage of a parallel query. In all-to-all aggregation, data is repartitioned on the GROUP BY attributes and every node aggregates a portion of the data. All-to-all aggregation is more common in the intermediate stages of a query plan.

In both all-to-one and all-to-all aggregations, directly transmitting the data to the destination node underutilizes the network. In all-to-one aggregation, only the receiving link of the destination and the sending links of the source nodes are used, while other network links are idle. The receiving link of the destination becomes the bottleneck. In all-to-all aggregation, workload imbalance due to skew or non-uniform networks [17] means that some network links will be underutilized when waiting for the slower or overburdened links to complete the repartitioning.

Systems such as Dremel [30], Camdoop [8], NetAgg [29] and SDIMS [52] reduce the communication cost and increase network utilization by using *aggregation trees* for all-to-one aggregations. The most relevant prior work is LOOM [9, 10], which builds aggregation trees with fixed fan-in. The main weakness of prior work is that it does not consider the *similarity* between datasets when building the aggregation tree. Figure 1 shows an example of an all-to-one aggregation. Assume a 4-node cluster, where  $v_R$  is the switch, node  $v_0$  is the destination node for this aggregation, node  $v_1$  stores three tuples with keys A, B and C, and nodes  $v_2$  and  $v_3$  store three tuples each with keys D, E and F. (For simplicity, the figures only show the GROUP BY keys.)

- The **repartitioning** strategy in Figure 2 finishes the aggregation in 9 time units, where a unit is the time it takes to receive and process a single tuple.
- The **similarity-aware** aggregation plan in Figure 3 proceeds in two phases. In the first phase,  $v_1$  transmits keys {A,B,C} to  $v_0$  and  $v_3$  transmits keys {D,E,F} to  $v_2$ . In the second phase,  $v_2$  computes the partial aggregation and transmits keys {D,E,F}. The entire aggregation completes in 6 time units — 1.5 $\times$  faster than repartitioning.

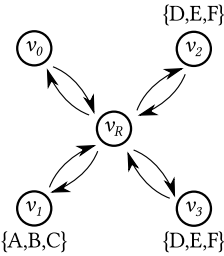


Figure 1: Graph representation of a cluster with four nodes. The aggregation destination is  $v_0$  and the router is  $v_R$ .

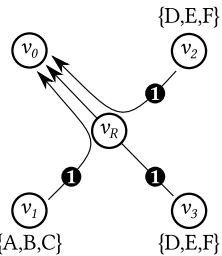
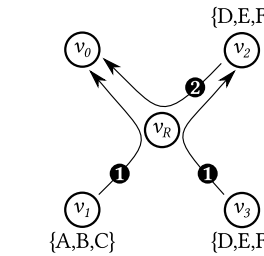
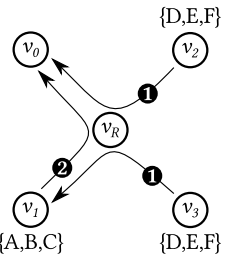


Figure 2: Aggregation based on **repartitioning** completes in 9 time units. The bottleneck is the  $v_R \rightarrow v_0$  link.



$P_1 = \{v_1 \rightarrow v_0, v_3 \rightarrow v_2\}$ ,  $P_2 = \{v_2 \rightarrow v_0\}$

Figure 3: The **similarity-aware** plan completes in 6 time units.



$P_1 = \{v_2 \rightarrow v_0, v_3 \rightarrow v_1\}$ ,  $P_2 = \{v_1 \rightarrow v_0\}$

Figure 4: The **similarity-oblivious** plan finishes in 9 time units.

- The **similarity-oblivious** aggregation plan shown in Figure 4 transmits keys  $\{D,E,F\}$  from  $v_3$  to  $v_1$  in the first phase and then needs 6 time units in the second phase to transmit keys  $\{A,B,C,D,E,F\}$  to  $v_0$ . The entire aggregation completes in 9 time units, as fast as repartitioning.

This paper introduces GRASP, an algorithm that carefully constructs aggregation trees to accelerate high-cardinality aggregation. Unlike prior solutions [30, 8, 29, 52] that are data-agnostic and do not consider how well can data be combined during the aggregation, GRASP *aggregates fragments with similar keys first to reduce the future network cost and thus improve performance*. GRASP has the following attributes: (1) it is distribution-aware as it selects aggregation pairs that will produce smaller partial aggregates, (2) it is topology-aware as it schedules larger data transfers on faster network links, (3) it achieves high network utilization as it attempts to use as many network links as possible.

The paper is structured as follows. Section 2 develops the theoretical model that GRASP uses to reason about the network cost of parallel data aggregation. Section 3 introduces GRASP, a topology-aware and data distribution-aware algorithm, that aims to reduce network cost by leveraging partition similarity during aggregation. A natural question to ask is if GRASP produces aggregation plans that have any theoretical guarantees on their optimality. Section 4 proves that the aggregation scheduling problem cannot be approximated within a constant factor by any polynomial algorithm (including GRASP), assuming the SSE conjecture. Section 5 contains the experimental evaluation with both synthetic and real data which shows that GRASP can be up to  $3.5\times$  faster than repartitioning and up to  $2.0\times$  faster than LOOM on real datasets.

Symbol	Description
$V_C$	A set of all compute nodes in the cluster
$s \rightarrow t$	Data transfer from node $s$ to node $t$
$P_i$	Phase $i$ , $P_i = \{s_1 \rightarrow t_1, s_2 \rightarrow t_2, \dots\}$
$\mathbb{P}$	Aggregation plan, $\mathbb{P} = \{P_1, P_2, \dots\}$
$X_i^l(v)$	Data of partition $l$ in node $v$ after $P_i$ completes
$X_i(v)$	Data in node $v$ after $P_i$ completes, $X_i(v) = \bigcup_l X_i^l(v)$
$X_0(v)$	Data in node $v$ before the aggregation starts
$X$	The entire dataset, $X = \bigcup_{v \in V_C} X_0(v)$
$Y_i(s \rightarrow t)$	Data sent from $s$ to $t$ in phase $P_i$
$w$	Size of one tuple
$B(s \rightarrow t)$	Available bandwidth for the $s \rightarrow t$ data transfer
$\text{COST}(s \rightarrow t)$	Network cost for the $s \rightarrow t$ data transfer
$\text{COST}(P_i)$	Network cost of phase $P_i$
$\text{COST}(\mathbb{P})$	Network cost of the aggregation plan $\mathbb{P}$

Table 1: Symbol definitions.

## 2. PROBLEM DEFINITION

We use a connected, directed, weighted graph  $G = (V(G), E(G))$  to represent the network topology of the cluster. Each edge  $\langle v_i, v_j \rangle \in E(G)$  represents one network link, with the edge direction to be the direction of data flow.

The fat-tree topology is widely used in data centers [1]. We represent all routers in the network as a single node  $v_R \in V(G)$  and model the fat-tree topology as a star network. The set  $V_C = V(G) - \{v_R\}$  represents the compute nodes of the cluster. Compute nodes have bidirectional network links, therefore  $E(G) = \{\langle s, v_R \rangle | s \in V_C\} \cup \{\langle v_R, t | t \in V_C\}$ , where edge  $\langle s, v_R \rangle$  represents the uplink and edge  $\langle v_R, t \rangle$  represents the downlink.

### 2.1 Modeling the all-to-one aggregation

**Aggregation Model.** We first consider an aggregation where data in the parallel database system is aggregated to one single node  $v^* \in V_C$ . Data is divided into  $m$  partitions,  $L = \{l_1, l_2, \dots, l_m\}$ . The aggregation consists of multiple phases which execute in serial order. We use  $\mathbb{P}$  to denote the aggregation execution plan which has  $n$  phases, with  $\mathbb{P} = \{P_1, P_2, \dots, P_n\}$ . Here  $P_i$  represents one phase of the aggregation. In a phase  $P_i$ , there are  $k$  concurrent data transfers,  $P_i = \{s_1 \rightarrow t_1, s_2 \rightarrow t_2, \dots, s_k \rightarrow t_k\}$ , where  $s_j \rightarrow t_j$  denotes the data transfer in which node  $s_j$  sends data to node  $t_j$ . We impose one constraint on the choice of  $s_j$  and  $t_j$  within one phase: a node can be both sending and receiving data in one phase, as long as it does not send and receive data belonging to the same partition. Figure 3 shows an aggregation execution plan  $\mathbb{P} = \{P_1, P_2\}$  with two phases. Phase  $P_1$  has two data transfers,  $P_1 = \{v_1 \rightarrow v_0, v_3 \rightarrow v_2\}$ , and phase  $P_2$  has one data transfer,  $P_2 = \{v_2 \rightarrow v_0\}$ .

The data in each compute node changes in every phase. We use  $X_i^l(v)$  to denote the data of partition  $l$  in node  $v$  after phase  $P_i$  completes.  $X_0^l(v)$  represents data of partition  $l$  in node  $v$  in the beginning of the aggregation execution.  $X_i(v) = \bigcup_{l \in L} X_i^l(v)$  represents the data in node  $v$  after phase  $P_i$  completes and  $X_0(v)$  is the data in node  $v$  in the beginning of the aggregation execution.  $Y_i(s \rightarrow t)$  denotes the data sent from  $s$  to  $t$  in the data transfer  $s \rightarrow t$  in phase  $P_i$ . A node can only send local data, hence  $Y_i(s \rightarrow t) \subseteq X_{i-1}(s)$ . After aggregation phase  $P_i$  completes,

$$X_i(v) = X_{i-1}(v) \bigcup \left( \bigcup_{s \rightarrow v \in P_i} Y_i(s \rightarrow v) \right) - \left( \bigcup_{v \rightarrow t \in P_i} Y_i(v \rightarrow t) \right) \quad (1)$$

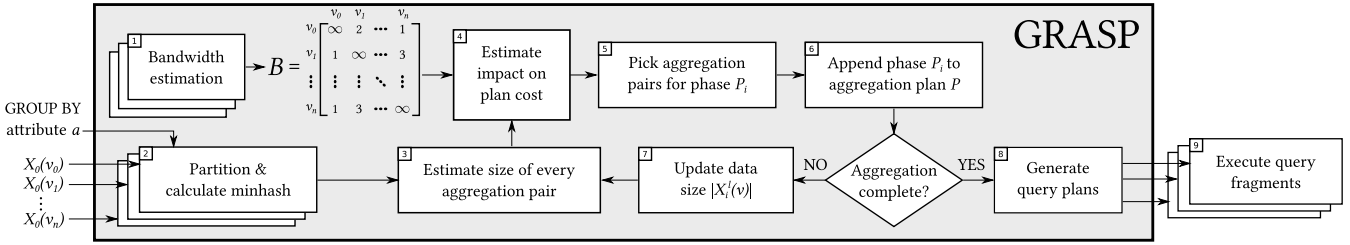


Figure 5: The GRASP framework.

The aggregation is complete when all nodes except  $v^*$  have sent their data out for aggregation.

$$\forall v \in V_C - \{v^*\} : X_n(v) = \emptyset \quad (2)$$

**Aggregation cost.** The aggregation execution plan  $\mathbb{P} = \{P_1, \dots, P_n\}$  consists of phases in serial order. Hence the network cost of  $\mathbb{P}$  is:

$$\text{COST}(\mathbb{P}) = \sum \text{COST}(P_i) \quad (3)$$

The network cost for phase  $P_i = \{s_1 \rightarrow t_1, s_2 \rightarrow t_2, \dots, s_k \rightarrow t_k\}$  is the cost of the network transfer which completes last:

$$\text{COST}(P_i) = \max_{s_j \rightarrow t_j \in P_i} \text{COST}(s_j \rightarrow t_j) \quad (4)$$

The cost for data transfer  $s_j \rightarrow t_j$  is the time it takes to transfer  $|Y_i(s_j \rightarrow t_j)|$  tuples of size  $w$  each over the available link bandwidth  $B(s_j \rightarrow t_j)$ :

$$\text{COST}(s_j \rightarrow t_j) = \frac{|Y_i(s_j \rightarrow t_j)| \cdot w}{B(s_j \rightarrow t_j)} \quad (5)$$

Section 3.2 shows how GRASP estimates  $B(s_j \rightarrow t_j)$  without network topology information. Section 4.1 shows how to calculate  $B(s_j \rightarrow t_j)$  when the network topology is known.

**Problem definition.** Given a connected, directed, weighted graph  $G$ , the final destination node  $v^* \in V$ , the data of each partition  $l \in L$  in each node  $X_0^l(v)$ , obtain an aggregation execution plan containing one or more phases  $\mathbb{P} = \{P_1, P_2, \dots, P_n\}$  such that  $\text{COST}(\mathbb{P})$  is minimized.

## 2.2 Modeling the all-to-all aggregation

This section extends the model defined for the all-to-one aggregation to capture the all-to-all aggregation.

**Aggregation Model.** In all-to-all aggregation every compute node in  $V_C$  is the aggregation destination for one or more partitions. This is specified by a mapping  $M : L \rightarrow V_C$  that maps a partition  $l \in L$  to a specific destination node  $v \in V_C$ . All-to-all aggregation completes when data in all partitions are aggregated to their corresponding destination:

$$\forall l \rightarrow v^* \in M : \forall v \in V_C - \{v^*\} : X_n^l(v) = \emptyset \quad (6)$$

**Problem definition.** Given a connected, directed, weighted graph  $G$ , the data of each partition  $l \in L$  in each node  $X_0^l(v)$ , and a mapping  $M : L \rightarrow V_C$ , obtain an aggregation execution plan containing one or more phases  $\mathbb{P} = \{P_1, P_2, \dots, P_n\}$  such that  $\text{COST}(\mathbb{P})$  is minimized.

## 3. THE GRASP FRAMEWORK

This section introduces GRASP, a GReedy Aggregation Scheduling Protocol, which uses partition similarity as a

heuristic to carefully schedule data transfers during aggregation to improve performance.

### 3.1 Overview

Figure 5 shows an overview of the GRASP framework. GRASP takes as inputs the data  $X_0(v)$  in every node  $v$  and the group by attribute  $a$ . The input data may be either a table in the database or an intermediate result produced during query processing. GRASP optimizes an aggregation in eight steps. Steps 1, 2 and 9 are run by all compute nodes, while steps 3–8 are run in the coordinator.

**1) Bandwidth estimation.** This step estimates the available bandwidth between any node pair and stores it as a matrix  $B$ . Section 3.2 describes the process in detail.

**2) Partition, pre-aggregate and calculate minhash signatures.** In this step every node partitions and aggregates data locally. During this operation, every node runs the minhash algorithm [3, 21, 14] to produce succinct minhash signatures.

**3) Estimate the result size of every possible aggregation pair.** The coordinator collects all the minhash signatures that were produced in step 2 and estimates the size of the result of all possible aggregation pairs. An aggregation pair is a partition  $l$ , a source node  $s$  and a destination node  $t$ . Section 3.3 presents the algorithms in detail.

**4) Estimate the impact on the cost of the final plan.** The coordinator takes the available bandwidth matrix  $B$  as input and uses it to estimate the runtime cost and the benefit of executing each possible aggregation pair. The cost function is described in Section 3.4.

**5) Generate aggregation phase  $P_i$ .** In this step, the coordinator selects all aggregation pairs for phase  $P_i$  based on their cost. The detailed algorithm is described in Section 3.5.

**6) Add  $P_i$  to aggregation plan  $\mathbb{P}$ .** The coordinator adds phase  $P_i$  to the aggregation plan  $\mathbb{P}$ , and outputs the current aggregation plan. If the aggregation is complete, the aggregation plan is scheduled for execution, otherwise the coordinator continues to Step 7.

**7) Update data size  $|X_i^l(v)|$ .** If the aggregation is not yet complete, the coordinator updates the estimation of the size of each partition  $|X_i^l(v)|$  in every node. Because the minhash calculation is composable, the minhash signature of the aggregation of two sets can be calculated from the minhash signatures of the two sets. Hence GRASP does not need to make another pass over the data to calculate the minhash signatures again.

**8) Generate query plans.** If the aggregation is complete, GRASP generates query plans and distributes them to each node for execution.

**9) Query execution.** In this step, every node in the cluster executes its assigned aggregations in every phase.

## 3.2 Estimating the bandwidth

This section describes how GRASP estimates the available bandwidth for data transfers without network topology information. GRASP schedules aggregation plans so that one node sends to and receives from at most one node within a phase to avoid network contention. This ensures that the outgoing link and the incoming link of each node are used by at most one data transfer. Similar approaches are used by Rödiger et al. [42] to minimize network contention.

GRASP measures the available bandwidth through a benchmarking procedure that is executed on system startup. Once the available bandwidth is estimated, it is stored in the bandwidth matrix  $B$  and is reused for all queries that follow. The bandwidth,  $B(s \rightarrow t)$ , is measured by running a benchmark on every  $s$  and  $t$  pair individually, where  $s$  keeps sending data to  $t$ . The average throughput is stored as the estimation of  $B(s \rightarrow t)$  in a matrix, where the row index is the sender and the column index is the receiver. (For example,  $B(v_0 \rightarrow v_1)$  is stored in location (0,1) and has throughput of 2 in Figure 5.) Section 5.3.1 evaluates the accuracy of the estimation and the robustness of GRASP to estimation errors.

## 3.3 Estimating the size of aggregation results

GRASP needs to estimate the size of an aggregation between nodes  $s$  and  $t$  for aggregation planning (described in Section 3.4). GRASP uses the minhash algorithm [3, 21, 14] for this estimation.

The minhash algorithm has three steps. (1) Generate the minhash signature for each partition. (2) Use the minhash signatures to estimate the Jaccard similarity between partitions, where Jaccard similarity  $J$  of sets  $S$  and  $T$  is defined as  $J = \frac{|S \cap T|}{|S \cup T|}$ . (3) Estimate the size of the result of an aggregation  $|S \cup T|$  from the Jaccard similarity.

Algorithm 1 calculates the minhash signature for a dataset. The minhash algorithm keeps  $n$  hash functions and applies the hash functions on every tuple in the partition. Each hash function produces one integer value. The values from the  $n$  hash functions constitute the *minhash signature*. Algorithm 1 is run by every compute node in step 1 in Figure 5. The minhash signatures are then sent to the coordinator.

Algorithm 2 shows how the coordinator estimates the size of aggregation results using the minhash signatures produced in Algorithm 1. The coordinator considers the size of the aggregation result for every possible transfer. The coordinator first estimates the Jaccard similarity of the two datasets with the minhash signature (Alg. 2 line 5) and then estimates the cardinality of the aggregation result (line 6). As the minhash signature of the aggregation result can be

**Algorithm 1:** The algorithm to generate minhash signatures in compute nodes.

---

**Input**  $X_0^l(s)$ : partition  $l$  in  $s$  before aggregation  
 $H = \{h_1(\cdot), h_2(\cdot), \dots, h_n(\cdot)\}$ : minhash functions  
**Output**  $\{S_1, S_2, \dots, S_n\}$ : the minhash signature of  $X_0^l(s)$

---

1 **for**  $h_i(\cdot) \in H$  **do**  
2    $S_i \leftarrow \min_{v \in X_0^l(s)} \{h_i(v)\}$

---

**Algorithm 2:** The algorithm to estimate aggregation result size from minhash signatures in the coordinator.

---

**Input**  $|X_i^l(s)|, |X_i^l(t)|$ : cardinality of partition  $l$  in  $s$  and  $t$  after completion of  $P_i$   
 $\{S_1, S_2, \dots, S_n\}$ : minhash signatures of  $X_i^l(s)$   
 $\{T_1, T_2, \dots, T_n\}$ : minhash signatures of  $X_i^l(t)$   
**Output**  $|X_i^l(s) \cup X_i^l(t)|$ : cardinality of  $X_i^l(s) \cup X_i^l(t)$   
 $\{(S \cup T)_1, (S \cup T)_2, \dots, (S \cup T)_n\}$ : the minhash signature of  $X_i^l(s) \cup X_i^l(t)$

---

1  $cnt \leftarrow 0$   
2 **for**  $j \in [1, n]$  **do**  
3   **if**  $S_j == T_j$  **then**  
4      $cnt \leftarrow cnt + 1$   
5  $J \leftarrow \frac{cnt}{n}$   
6  $|X_i^l(s) \cup X_i^l(t)| \leftarrow \frac{1}{1+J} \cdot (|X_i^l(s)| + |X_i^l(t)|)$   
7 **for**  $j \in [1, n]$  **do**  
8    $(S \cup T)_j \leftarrow \min(S_j, T_j)$

---

calculated from the minhash signature of the two datasets, Algorithm 1 needs to run only once and not after every aggregation phase. Instead, the coordinator updates the cardinality of data partitions with the estimation from the minhash estimation in the following phases (step 7 in Figure 5).

A natural question is how many hash functions does minhash need to be accurate. Fortunately, a minhash signature with as little as  $n = 100$  values (less than 1KB) suffices: Satuluri and Parthasarathy [44] show that the estimation is within 10% of the accurate similarity with probability larger than 95% for all values of  $J$  when  $n = 100$ . Section 5.3.4 evaluates the accuracy of the minhash estimation in practice.

## 3.4 Balancing cost and benefit

We turn to heuristics to minimize the cost of aggregation plans produced by GRASP. Ideally GRASP needs to take the cost of all aggregation phases into account when picking the best plan. However, this is prohibitively expensive as there are  $n^{n-2}$  plans for a cluster with  $n$  nodes [4]. At the other extreme, one can minimize the cost of the current phase, however this greedy approach will only schedule aggregations which transfer less data and will not utilize similarity to save on future data transfers. GRASP uses a heuristic that only considers two phases: the current and the next.

In GRASP, each data transfer transmits data belonging in one partition. For a candidate aggregation  $s \rightarrow t$  in phase  $P_i$ , where  $s$  sends out partition  $X_{i-1}^{l_1}(s)$  to aggregate with partition  $X_{i-1}^{l_2}(t)$  in  $t$ , the cost of the aggregation in the current phase is  $\text{COST}(s \rightarrow t)$ , where  $Y_i(s \rightarrow t) = X_{i-1}^{l_1}(s)$ . The cost of the next phase of aggregation is minimized by minimizing  $|X_{i-1}^{l_1}(s) \cup X_{i-1}^{l_2}(t)|$  which is the size of the aggregation result. (Section 3.3 describes how to estimate  $|X_{i-1}^{l_1}(s) \cup X_{i-1}^{l_2}(t)|$ ). We define a heuristic function  $C_i(s, t, X_{i-1}^{l_1}(s), X_{i-1}^{l_2}(t))$  for the candidate aggregation  $s \rightarrow t$  based on the following intuition:

- 1) One needs to minimize the cost of the aggregation  $s \rightarrow t$  which is  $\text{COST}(s \rightarrow t)$ . We also need to minimize the size of the aggregation result, which is to minimize  $|X_{i-1}^{l_1}(s) \cup X_{i-1}^{l_2}(t)|$  so as to minimize the cost of subsequent phases.

	$v_0$	$v_1$	$v_2$	$v_3$
$v_0$	$\infty$	$\infty$	$\infty$	$\infty$
$v_1$	3	$\infty$	9	9
$v_2$	3	9	$\infty$	6
$v_3$	3	9	6	$\infty$

Figure 6: The matrix  $C_1$  for the phase  $P_1$  of the aggregation problem in Figure 1. We assume  $w$  to be 1 unit and bandwidth to be 1 unit. The row ID is the node sending data and the column ID is the node receiving data. The circled 6 represents the aggregation  $v_2 \rightarrow v_3$  and  $v_2$  sends out  $\{D, E, F\}$  to aggregate with  $\{D, E, F\}$  in  $v_3$ .

We define  $E_i(s \rightarrow t, X_{i-1}^{l_1}(s), X_{i-1}^{l_2}(t)) = \frac{|X_{i-1}^{l_1}(s) \cup X_{i-1}^{l_2}(t)| \cdot w}{B(s \rightarrow t)}$  to assist in the definition of the heuristic metric. We seek to minimize the metric  $C_i(s, t, X_{i-1}^{l_1}(s), X_{i-1}^{l_2}(t)) = \text{COST}(s \rightarrow t) + E_i(s \rightarrow t, X_{i-1}^{l_1}(s), X_{i-1}^{l_2}(t))$ .

2) A special case is  $t = M(l_1)$ , where  $M(l_1)$  is the final destination node for the partition  $l_1$ : data sent to  $t$  does not need to be transmitted again as it has reached its final destination. Hence, we set  $C_i$  to  $\text{COST}(s \rightarrow t)$  in this case.

3) GRASP excludes the following aggregations in its heuristic by setting  $C_i$  to infinity so that they will never be picked: (1) Node  $s$  sending partitions whose destination is  $s$ , to prevent circular transmissions. (2) One node sending a partition to itself, as this is equivalent to a no-op. (3) Aggregations which involve nodes that neither have data for this partition nor are they the final destination for this partition, as no data would be aggregated in this operation. (4) Aggregating data in different partitions, as different partitions do not have common keys and thus no data would be aggregated.

Based on the above intuition, we construct matrix  $C_i$  to represent the total impact of every candidate aggregation for phase  $P_i$  as follows:

$$C_i(s, t, X_{i-1}^{l_1}(s), X_{i-1}^{l_2}(t)) = \begin{cases} \text{COST}(s \rightarrow t) & t = M(l_1) \wedge X_{i-1}^{l_1}(s) \neq \emptyset \\ \infty & s = t \\ \infty & s = M(l_1) \\ \infty & l_1 \neq l_2 \\ \infty & X_{i-1}^{l_1}(s) = \emptyset \\ \infty & X_{i-1}^{l_2}(t) = \emptyset \\ \text{COST}(s \rightarrow t) + E_i(s \rightarrow t) & \text{otherwise} \end{cases} \quad (7)$$

Figure 6 shows the matrix  $C_1$  for the phase  $P_1$  of the aggregation problem in Figure 1. There is only one partition in each node. The row index is the sending node and the column index is the receiving node. Note that the matrix  $C_i$  is not symmetric, because the aggregations  $s \rightarrow t$  and  $t \rightarrow s$  transfer different data and use different network links.

### 3.5 Aggregation selection heuristic

This section describes step 5 in Figure 5 which selects among candidate aggregations to generate one phase of aggregation. The goal is to minimize the overall cost of the whole aggregation plan  $\mathbb{P}$ . There are three aspects for consideration when selecting candidate aggregations:

1) How many aggregations does one node participate in one phase? Prior work [42, 43] shows that uncoordinated network communication leads to congestion in the network. Rödiger et al. [42] do application-level network scheduling by dividing communication into stages to improve throughput, where in each stage a server has one target to send to and a single source to receive from. Like prior work, GRASP restricts the communication within one phase such that one node sends to at most one node and receives from at most one node, in order to minimize network contention.

2) How many nodes are selected for aggregation in one phase? In order to maximize the network utilization, GRASP picks as many data transfers as possible in one phase until the available bandwidth  $B$  is depleted.

3) Given many candidate aggregation pairs, which aggregation should one choose within one phase? GRASP selects aggregations by consulting the  $C_i$  metric that was defined in Equation 7 and tries to pick aggregations with the smallest  $C_i$  values.

The algorithm to select candidate aggregations for one phase is shown in Algorithm 3.  $V_{send}$  is the set of candidate senders,  $V_{recv}$  is the set of candidate receivers,  $V_{l_j}$  is the set of candidate nodes for partition  $l_j$ . The algorithm picks the candidate aggregation pair which has smallest value of the metric (line 3), remove the nodes from the candidate node sets (line 4) so as to enforce the requirement that one node only sends to and receives from at most one node and does not send and receive data in the same partition within the same phase. The candidate aggregation is added to the aggregation phase (line 7). The algorithm stops when either the candidate set has no nodes (line 2) or there is no valid candidate aggregations (line 6).

Figure 7 shows an example of how GRASP selects aggregations from the  $C_i$  matrix. For simplicity, we show an all-to-one aggregation with a single partition, and we assume the bandwidth  $B$  to be equal to the tuple width  $w$ . In the first iteration, the coordinator constructs the metric matrix  $C_1$  from the heuristic function described in Section 3.4. For example, if in the first iteration,  $|X_0(v_2)| = 3$ ,  $|X_0(v_2) \cup X_0(v_3)| = 3$ , with  $B(v_2 \rightarrow v_3) = w$  we get  $C_1(v_2, v_3, X_0(v_2), X_0(v_3)) = 6$ . After constructing the metric matrix  $C_1$ , GRASP picks data transfers for aggregation

---

**Algorithm 3:** The algorithm to pick data transfers for aggregation within one phase

---

**Input**  $C_i$ : the cost metric used in the heuristic  
 $V_{send}$ : the candidate node set for sender  
 $V_{recv}$ : the candidate node set for receiver  
 $V_{l_j}$ : the candidate node set for partition  $l_j$

**Output**  $P_i$ : one phase of aggregation

- 1  $P_i \leftarrow \emptyset$ ,  $V_{send} \leftarrow V_C$ ,  $V_{recv} \leftarrow V_C$ ,  $V_{l_j} \leftarrow V_C$
- 2 **while**  $|V_{send}| > 1$  and  $|V_{recv}| > 1$  **do**
- 3     Pick  $\langle s \rightarrow t, X_{i-1}^{l_1}, X_{i-1}^{l_2} \rangle$  s.t.  
 $s \in V_{send}$ ,  $t \in V_{recv}$ ,  $s \in V_{l_1}$ ,  $t \in V_{l_2}$  and  
 $C_i(s, t, X_{i-1}^{l_1}, X_{i-1}^{l_2})$  has minimum value in  $C_i$
- 4     Remove  $s$  from  $V_{send}$  and  $V_{l_1}$ ,  $t$  from  $V_{recv}$  and  $V_{l_2}$
- 5     **if**  $C_i(s, t, X_{i-1}^{l_1}, X_{i-1}^{l_2}) = \infty$  **then**
- 6         **break**
- 7     Add  $\langle s \rightarrow t, X_{i-1}^{l_1}, X_{i-1}^{l_2} \rangle$  to  $P_i$

---

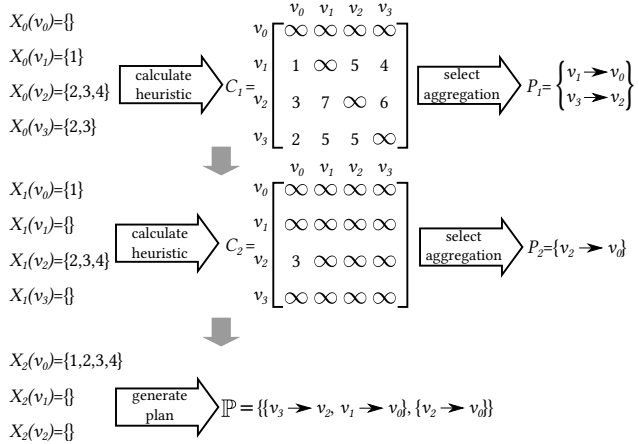


Figure 7: An example of how GRASP generate aggregation plans for an all-to-one aggregation with one single partition.

using Algorithm 3.  $v_1 \rightarrow v_0$  is first picked because it has the least cost. As a transfer has now been scheduled on the  $v_1 \rightarrow v_0$  link, GRASP eliminates  $v_1$  and  $v_0$  from all candidate sets. GRASP then picks  $v_3 \rightarrow v_2$ . GRASP then finishes this phase because there are no candidates left, and produces the aggregation phase  $P_1 = \{v_1 \rightarrow v_0, v_3 \rightarrow v_2\}$ . GRASP continues until all data has been aggregated to the destination nodes.

## 4. HARDNESS OF APPROXIMATION

Many hard problems are amenable to efficient approximation algorithms that quickly find solutions that are within a guaranteed distance to the optimal. For instance, 2-approximation algorithms—polynomial algorithms that return a solution whose cost is at most twice the optimal—are known for many NP-hard minimization problems. A natural question to ask is how closely does GRASP approximate the optimal solution to the aggregation problem.

This section proves that it is not feasible to create a polynomial algorithm that approximates the optimal solution to the aggregation problem within any constant factor. In other words, the aggregation problem is not only NP-hard but it also cannot be approximated within any constant factor by any polynomial algorithm, including GRASP. This hardness of approximation result is much stronger than simply proving the NP-hardness of the problem, as many NP-hard problems are practically solvable using approximation.

The proof is structured as follows. Section 4.1 introduces a necessary assumption regarding the cost of using shared network links. Section 4.2 defines the Small Set Expansion (SSE) problem and the well-established SSE conjecture. Section 4.3 starts with an instance of SSE and reduces it to the all-to-one aggregation problem. This proves that the all-to-one aggregation problem is NP-hard to approximate, assuming the SSE conjecture. Section 4.3.3 proves that the all-to-all aggregation problem is also NP-hard to approximate.

### 4.1 Link sharing assumption

Whereas GRASP will never schedule concurrent data transfers on the same link in one phase in a star network, the theoretical proof needs a mechanism to assess the runtime cost

of sharing a network link for multiple transfers. Our proof makes the fair assumption that the cost of sending data from one node to another node is proportional to the total data volume that is transferred over the same link across all aggregations in this phase.

One way to incorporate link sharing information in the cost calculation is to account for the number of concurrent data transfers on the  $s \rightarrow t$  path when computing the available bandwidth  $B(s \rightarrow t)$ . For example, for the network topology shown in Figure 1 the available bandwidth from  $s$  to  $t$ ,  $B(s \rightarrow t)$  can be calculated as:

$$B(s \rightarrow t) = \min \left( \frac{W(s, v_R)}{d_o(s)}, \frac{W(v_R, t)}{d_i(t)} \right) \quad (8)$$

where  $W(s, v_R)$  and  $W(v_R, t)$  is the network bandwidth of the links,  $d_o(s)$  denotes the number of data transfers using the  $(s, v_R)$  link and  $d_i(t)$  denotes the number of data transfers using the  $(v_R, t)$  link in this phase.

## 4.2 The Small Set Expansion Problem

This sub-section defines the Small Set Expansion (SSE) conjecture that was introduced by Raghavendra and Steurer [37]. We first briefly discuss the intuition behind this problem and we then give a formal definition.

### 4.2.1 Intuition

A  $d$ -regular graph is a graph where each vertex has  $d$  edges for some integer  $d \geq 1$ . The Small Set Expansion problem asks if there exists a small subset of vertices that can be easily disconnected from the rest in a  $d$ -regular graph. The SSE conjecture states that it is NP-hard to distinguish between the following two cases: (1) The **YES** case, there exists some small set of vertices that can be disconnected from the graph. (2) The **NO** case, such a set does not exist. In other words, every set of vertices has a relatively large boundary to the other vertices in the graph.

Note that the SSE conjecture is currently open, as it has not been proven or disproven yet. Just like with the well-known  $\mathbf{P} \neq \mathbf{NP}$  conjecture, the theory community has proceeded to show that many problems are hard to approximate based on the general belief that the SSE conjecture is true. Significant hardness of approximation results that assume the SSE conjecture include the treewidth and pathwidth of a graph [2], the Minimum Linear Arrangement (MLA) and the  $c$ -Balanced Separator problem [38].

### 4.2.2 Background

The formulation of the Unique Game Conjecture, UGC, introduced a valuable tool to resolve the complexity of many optimization problems [23]. Despite the introduction of UGC, it remained elusive whether certain graph problems were amenable to approximation. Despite this progress, the approximation result for certain graph expansion problems such as Minimum Linear Arrangement (MLA) problem and  $c$ -Balanced Separator problem remained unresolved. This means that even assuming the UGC, this is not sufficient to obtain a hardness of approximation for these problems. Furthermore, the approximation status of many other graph layout problems is not clarified, even assuming the UGC. In 2010, Raghavendra and Steurer introduced the Small Set Expansion (SSE) conjecture [37] which implies the UGC. It has been shown that the SSE conjecture implies the hardness

of approximation for MLA and  $c$ -Balanced Separator problem [38]. Many hardness of approximation results have been obtained using the SSE conjecture, including the hardness of approximating the treewidth and pathwidth of a graph [2], that were out of reach of UGC. Furthermore, they show that a variety of different graph layout problems are hard to approximate. These results show that the SSE conjecture serves as a natural conjecture that not only implies the UGC but also shows hardness of approximation for several problems that are out of reach of the UGC. We are going to state this conjecture, and assuming it, we will be proving the hardness of approximation for the aggregation scheduling problem.

#### 4.2.3 Formal Definition

Let  $G$  be an undirected  $d$ -regular graph. For any subset of vertices  $S \subseteq V(G)$ , we define the *edge expansion* of  $S$  to be  $\Phi(S) = \frac{|E(S, V \setminus S)|}{d|S|}$ .

**Definition 4.1.** Let  $\rho \in [-1, 1]$ . Let  $\Phi^{-1}$  be the inverse function of the normal distribution. Let  $X$  and  $Y$  be jointly normal random variables with mean 0 and covariance matrix  $\begin{pmatrix} 1 & \rho \\ \rho & 1 \end{pmatrix}$ . We define  $\Gamma_\rho: [0, 1] \rightarrow [0, 1]$  as  $\Gamma_\rho(\mu) = \Pr[X \leq \Phi^{-1}(\mu) \wedge Y \leq \Phi^{-1}(\mu)]$ .

**Conjecture 4.2** (The Small Set Expansion conjecture [37]). For every integer  $q > 0$  and  $\varepsilon, \gamma > 0$ , it is NP-hard to distinguish between the following two cases:

**YES** There is a partition of  $V(G)$  into  $q$  equi-sized sets  $S_1, \dots, S_q$  such that  $\Phi(S_i) \leq 2\varepsilon, \forall i \in \{1, \dots, q\}$ .

**NO** For every  $S \subseteq V(G)$  we have  $\Phi(S) \geq 1 - (\Gamma_{1-\varepsilon/2}(\mu) + \gamma)/\mu$ , where  $\mu = |S|/|V(G)|$ .

**Remark 4.1.** In the **YES** case, the total number of edges that are not contained in one of the  $S_i$  sets is at most  $2\varepsilon|E|$ .

**Remark 4.2.** In the **NO** case, for every  $S \subseteq V(G)$  with  $|V(G)|/10 \leq |S| \leq 9|V(G)|/10$ , we have  $|E(S, V(G) \setminus S)| \geq c\sqrt{\varepsilon}|E(G)|$ , for some constant  $c > 0$ .

### 4.3 Hardness of the aggregation problem

Before stating the formal inapproximability result, we first provide the intuition behind our proof strategy approach. We then reduce the SSE problem to the all-to-one aggregation problem. Finally, we show that the all-to-all problem is a straightforward generalization of the all-to-one problem.

#### 4.3.1 Intuition

We now give a brief intuitive overview of the proof. Recall that in the SSE problem we are given a graph  $G$  and the goal is to decide whether  $G$  admits a partition into small subgraphs, each having small boundary (a SSE partition henceforth), or  $G$  is an expander at small scales; that is, all small subgraphs of  $G$  have large boundary. The SSE conjecture asserts that this problem is hard to approximate, and has been used to show the inapproximability of various graph optimization problems [2]. Inspired by these results, we show that the all-to-one aggregation problem is hard to approximate by reducing the SSE problem to it. Our proof strategy is as follows. We begin with an instance  $G'$  of the SSE problem. We encode  $G'$  as an instance of the all-to-one aggregation problem by interpreting each node of  $G'$  as a leaf node in the star aggregation network, and each edge  $u, v$  of

$G$  as a data item which is replicated in nodes  $u$  and  $v$  in the aggregation problem. We show that any partition of  $G$  can be turned into an aggregation protocol, and, conversely, any aggregation protocol can be turned into a partition of  $G$ . The key intuition is that the cost of the partition is related to the cost of the aggregation via the observation that the data items that need to be transmitted twice are exactly the edges that are cut by the partition.

#### 4.3.2 Formal proof for the all-to-one aggregation

Suppose that we are given an all-to-one aggregation instance: a graph  $G$ , a single destination vertex  $v^* \in V(G)$ , and the data  $X_0(v)$  in each node  $v \in V(G)$ . Let  $X = \bigcup_{v \in V(G)} X_0(v)$  be the set of all data. Let  $\mathbb{P} = \{P_1, P_2, \dots, P_n\}$  be an execution plan. For every  $P_i = \{s_1 \rightarrow t_1, \dots, s_k \rightarrow t_k\} \in \mathbb{P}$ , let  $S(P_i) = \{s_1, \dots, s_k\}$  and  $T(P_i) = \{t_1, \dots, t_k\}$ .

We define the *overhead cost* of  $\mathbb{P}$  to be  $\text{COST}(\mathbb{P}) - |X|$ . Under the all-to-one aggregation model, every execution plan is obtained from an aggregation tree. To simplify the proof, we assume that one node sends data to only one node within a phase. This modeling assumption is acceptable from a theoretical standpoint as one can represent a phase where a node transmits data to multiple destinations as a sequence of discrete phases to each individual destination. We say that  $\mathbb{P}$  is obtained from an *aggregation tree*  $T_P$ , if the following conditions hold:

1.  $T_P$  is a spanning tree of  $G$ , rooted at  $v^*$ .
2. The leaf vertices of  $T_P$  are exactly the elements of  $S(P_1)$ . Furthermore, for every  $i \in \{2, \dots, k-1\}$ , the leaf vertices of  $T_P \setminus \bigcup_{1 \leq j < i} S(P_j)$  are exactly the elements of  $S(P_i)$ .

**Theorem 4.3.** For every  $\varepsilon > 0$ , given an aggregation instance  $(G, v^* \in V(G), X_0(v) \forall v \in V(G))$ , it is SSE-hard to distinguish between the following two cases:

**YES** There exists an execution plan that is obtained from an aggregation tree with overhead cost  $O(\varepsilon|X|)$ .

**NO** Every execution plan that is obtained from an aggregation tree has overhead cost  $\Omega(\sqrt{\varepsilon}|X|)$ .

*Proof.* We start with an instance of SSE with  $q = 1/\varepsilon$ , and reduce it to our problem. Let  $G'$  be the  $d$ -regular graph of the SSE instance. We construct an aggregation instance as follows. Let  $V(G) = V(G')$ , and  $X = E(G')$ . Note that  $G$  is a complete graph with the same vertex set as  $G'$ . For every  $v \in V(G)$ , let  $X_0(v) = \{\{u, w\} \in X : v = u \vee v = w\}$  be the set of data that is held by  $v$ .

In the **YES** case of the SSE instance, we have disjoint sets  $S_1, S_2, \dots, S_q$  of equal size. For every  $i \in \{1, 2, \dots, q\}$ , we have  $|S_i| = |V(G)|/q = \varepsilon|V(G)|$ . We may assume w.l.o.g. that  $v^* \in S_q$ . For every  $i \in \{1, 2, \dots, q-1\}$ , pick an arbitrary vertex  $v_i \in S_i$ . Let also  $v_q = v^*$ . For every  $j \in \{1, 2, \dots, q\}$ , let  $\{s_{i,1}, \dots, s_{i,i_j}\} = S_j \setminus \{v_j\}$ . We first construct an aggregation tree  $T$  as follows. For every  $i \in \{1, 2, \dots, q\}$ , let  $v_i$  be the parent of all other vertices in  $S_i$ . Let  $v_q$  be also the parent of  $v_1, v_2, \dots, v_{q-1}$ .

Now consider the execution plan corresponding to  $T$ . This aggregation has two phases:  $\mathbb{P} = \{P_1, P_2\}$ . First we describe  $P_1$ . For each  $S_i$ , we aggregate all the data held by vertices of  $S_i$  to  $v_i$ ; that is every vertex in  $S_i$  (except  $v_i$  itself), transfers its dataset to  $v_i$ . This can be done simultaneously for all  $S_i$ 's, since  $S_i$ 's are disjoint sets. We have that  $P_1 = \{s_{1,1} \rightarrow v_1, s_{1,2} \rightarrow v_1, \dots, s_{1,i_1} \rightarrow v_1, s_{1,2} \rightarrow v_2, \dots, s_{1,i_2} \rightarrow v_2, \dots, s_{q,1} \rightarrow v_q, \dots, s_{q,i_q} \rightarrow v_q\}$ .

By the construction, at the beginning for each vertex  $v$  we have that  $|X_0(v)| = d$ . Therefore, for every  $S_i$ , the total volume of data to be transferred to  $v_i$  is  $2\varepsilon|E(G)| = d\varepsilon|V(G)| = d|S_i|$ . In other words, for every  $(s_{i,j} \rightarrow v_i) \in P_1$ , we have that  $\text{COST}(s_{i,j} \rightarrow v_i) = 2\varepsilon|E(G)|$ , and thus we have  $\text{COST}(P_1) = 2\varepsilon|E(G)|$ .

In the second phase of the execution plan, for every  $i \in \{1, 2, \dots, q-1\}$ , we need to transfer all the data held by  $v_i$  to  $v^*$ . This can be done simply by sending one data at a time to  $v^*$ . We have:

$$P_2 = \{v_1 \rightarrow v_q, v_2 \rightarrow v_q, \dots, v_{q-1} \rightarrow v_q\}$$

By Remark 4.1, the total number of data that are transferred more than once in this phase is at most  $\varepsilon d|V(G)| = 2\varepsilon|E(G)|$ . This means that  $\text{COST}(P_2) \leq (1 + 2\varepsilon)|E(G)|$ . Therefore we have that  $\text{COST}(\mathbb{P}) \leq (1 + 4\varepsilon)|E(G)|$ , and thus the overhead cost of this execution plan is  $O(\varepsilon|E(G)|)$ , as desired.

In the **NO** case, we want to show that every execution plan that is obtained from an aggregation tree has cost  $\Omega(\sqrt{\varepsilon}|E|)$ . Let  $\mathbb{P}$  be an execution plan that is obtained from an aggregation tree  $T$ . For every  $v \in V(T)$ , let  $T_v$  be the subtree of  $T$  rooted at  $v$ .

Suppose that  $v^*$  has a child  $v$  such that  $|V(T)|/10 \leq |V(T_v)| \leq 9|V(T)|/10$ . We apply Remark 4.2 by setting  $S = T_v$ . We have that  $|E(S, V(G) \setminus S)| \geq c\sqrt{\varepsilon}|E(G)|$ , for some constant  $c > 0$ . This means that there are at least  $c\sqrt{\varepsilon}|E(G)|$  data that are going to be sent at least twice to  $v^*$  in the execution plan, or  $\text{COST}(\mathbb{P}) = \Omega((1 + \sqrt{\varepsilon})|E(G)|)$ . Thus, the overhead cost of this execution plan is  $\Omega(\sqrt{\varepsilon}|E(G)|)$ , as desired.

Otherwise,  $v^*$  has a child  $v$  such that  $|V(T_v)| < |V(T)|/10$ . In this case, there are at least  $9|E(G)|/10$  data in  $T_v$  that are going to be transferred at least twice to get to  $v^*$  in the execution plan. Therefore, we have  $\text{COST}(\mathbb{P}) = \Omega((0.9 + 0.9)|E(G)|)$ , and thus the overhead cost of this execution plan is  $\Omega(0.8|E(G)|)$  which is clearly  $\Omega(\sqrt{\varepsilon}|E(G)|)$ . This completes the proof.  $\square$

**Corollary 4.4.** *Assuming Conjecture 4.2, it is NP-hard to approximate the minimum overhead cost of an all-to-one aggregation plan that is obtained from an aggregation tree within any constant factor.*

**Corollary 4.5.** *Assuming Conjecture 4.2, it is NP-hard to find an all-to-one aggregation plan that is obtained from an aggregation tree with minimum cost.*

One might ask if it is feasible to brute-force the problem for small graphs by enumerating all possible aggregation trees and picking the best solution. Unfortunately this would be extremely expensive even for small graphs. Cayley's formula [4] states that the number of different spanning trees of graph with  $n$  vertices is  $n^{n-2}$ . Hence, even for  $n = 20$  one needs to enumerate  $20^{18} \geq 10^{23}$  different trees.

### 4.3.3 Formal proof for the all-to-all aggregation

The more general case is the all-to-all aggregation problem. We observe that the all-to-one aggregation problem can be trivially reduced to the all-to-all aggregation problem, since by the definition, every instance of the all-to-one aggregation problem is also an instance of the all-to-all aggregation problem.

**Theorem 4.6.** *Assuming Conjecture 4.2, it is NP-hard to find an all-to-all aggregation plan with minimum cost.*

*Proof.* We reduce the all-to-one aggregation problem to the all-to-all aggregation problem. Suppose that we are given an instance of the all-to-one aggregation problem. By its definition, this is also an instance of the all-to-all aggregation problem where the mapping  $M$  is such that the aggregation destination of every partition is node  $v^* \in V_C$ . By Corollary 4.5 we know that the all-to-one aggregation problem is NP-hard assuming Conjecture 4.2, therefore the all-to-all aggregation problem is NP-hard as well, as desired.  $\square$

## 5. EXPERIMENTAL EVALUATION

In this section, we compare the GRASP algorithm with the repartition algorithm and LOOM. Section 5.1 introduces the experiment setup, which includes the hardware setting, the workloads and the baselines. The other sections evaluate the following questions:

- (§ 5.2.1) How well does GRASP leverage similarity between datasets?
- (§ 5.2.2) How does similarity within the dataset affect performance?
- (§ 5.2.3) Can GRASP benefit from workload imbalance?
- (§ 5.3.1) How accurate is the bandwidth estimation? How robust is GRASP to estimation errors?
- (§ 5.3.2) How does GRASP perform in non-uniform networks?
- (§ 5.3.3) How does the performance change when the number of fragments increases?
- (§ 5.3.4) Is GRASP faster than aggregation based on repartitioning and LOOM on TPC-H and real datasets?
- (§ 5.3.5) How well does GRASP work in a real-world deployment where the network conditions are unpredictable?

### 5.1 Experiment setup

We implemented the GRASP framework in C++ with about 3000 lines of code. We evaluate GRASP in two clusters. The first is a shared cluster connected by a 1 Gbps network. Each machine has two Intel Xeon E5-2680v4 14-core processors and 512 GB of memory. The second cluster is Amazon EC2 with d2.8xlarge instances which have 36 vCPUs and 244 GB of memory. The instances are connected with a 10 Gbps network. We run one or multiple aggregation fragments in each machine/instance. Hence, one fragment corresponds to one logical graph node in Section 2.

Our evaluation reports the total response time to complete the aggregation query, which includes the time to plan the aggregation using GRASP, the time to transfer the data and the time to process the aggregation in each node. All experiments use hash-based local aggregation.

#### 5.1.1 Baselines

We compare GRASP with two baselines. The first baseline is LOOM [9, 10]. LOOM uses the size of the final aggregation output and the size of the aggregation result of

one single fragment in query planning. While getting the accurate size of aggregation results is unrealistic, we use the accurate size in LOOM so that LOOM achieves its best performance. The second baseline is repartition which has two versions. One version is without local aggregation, where data is directly sent to the destination fragment for aggregation. We use “Repart” to denote this version. The other version is with local aggregation, where data is first aggregated locally, then the local aggregation result is sent to the destination fragment for aggregation. We use “Preagg+Repart” to denote this version of repartition. Notice that repartition works for both all-to-all and all-to-one aggregations, while LOOM only works for all-to-one aggregations.

### 5.1.2 Workloads

We use five workloads in our evaluation.

**1) Synthetic workload.** The first workload is a synthetic workload which has one table  $R$ , with two long integers  $R.a$  and  $R.b$  as attributes. The query evaluated is `SELECT R.a SUM(R.b) FROM R GROUP BY R.a`.

**2) TPC-H workload.** The second workload is the TPC-H workload with scale factor 80. We evaluate the subquery in TPC-H Q18. `SELECT ORDERKEY, SUM(QUANTITY) FROM LINEITEM GROUP BY ORDERKEY`. The LINEITEM table is partitioned and distributed on the SUPPKEY to fragments with a modulo hash function.

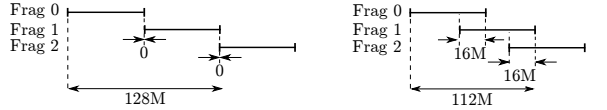
**3) MODIS workload.** The third workload is the Surface Reflectance data MOD09 from MODIS (Moderate Resolution Image Spectroradiometer) [47]. The MODIS data provides the surface reflectance of 16 bands together with the location coordinates (latitude and longitude). In the processing of MODIS data, one product is MOD09A1 [48] which aggregates the observed data in an 8-day period with the following query: `SELECT Latitude, Longitude, MIN(Band3) FROM ReflectTable GROUP BY ROUND(Latitude, 2), ROUND(Longitude, 2) WHERE Date BETWEEN '01/01/2017' AND '01/08/2017'`. The MODIS data is stored in separate files, one file per satellite image in timestamp order. We download about 1200 files from the MODIS website, and assigned files into plan fragments in a round-robin fashion. Overall, there are about 3 billion tuples and 648 million distinct GROUP BY keys in this dataset.

**4) Amazon workload.** The fourth dataset is the Amazon review dataset [19]. The review dataset has more than 82 million reviews from about 21 million users. The dataset includes the reviewer ID, overall rating, review time and detail review etc. We evaluate the following query to calculate the average rating a customer gives out. `SELECT ReviewerID, AVG(OverallRate) FROM AmazonReview GROUP BY ReviewerID`. The reviews are stored in timestamp order and we split this file into plan fragments.

**5) Yelp workload.** The fifth dataset is the yelp review dataset [54]. The review dataset has more than 5 million reviews from about 1.3 million users. The yelp dataset has similar attributes as the Amazon dataset and we use a similar query as in the Amazon workload to calculate the average stars a customer gives.

## 5.2 Experiments with uniform bandwidth

In this section, we evaluate GRASP with uniform bandwidth between fragments, where each plan fragment communicates with the same bandwidth. The measured bandwidth is 118 MB/s. We experiment with 8 machines and 1 frag-



(a) Jaccard similarity  $J = \frac{0}{128}$ . (b) Jaccard similarity  $J = \frac{16}{112}$ .

Figure 8: The line segments represent the range of GROUP BY attributes. The Jaccard similarity increases when the overlap of GROUP BY key ranges increases.

ment per machine, which is 8 fragments in total. We use the synthetic workload in this section.

### 5.2.1 Effect of similarity across fragments

GRASP takes advantage of the similarities between datasets in different fragments in aggregation scheduling. How well does the GRASP algorithm take advantage of similarities between datasets?

In this experiment, we change the similarities between datasets, i.e. the number of common GROUP BY keys, in different plan fragments. Each plan fragment has 64 million tuples. Figure 8 shows how we change the similarity between datasets. Each segment in Figure 8 shows the range of  $R.a$  in one fragment. Here we only show fragment 0, 1 and 2 for space. The range of datasets between adjacent fragments has an overlap. The Jaccard similarity increases when the size of overlap increases.

The experiment results for all-to-one aggregation are shown in Figure 9. The horizontal axis is the Jaccard similarity coefficient between datasets. The vertical axis is the speedup over the Preagg+Repart algorithm with Jaccard similarity 0. Here speedup 1 corresponds to response time of 64.6 seconds. Figure 9 shows that GRASP has the best performance and is up to  $4.1 \times$  faster than Preagg+Repart and  $2.2 \times$  faster than LOOM when the Jaccard similarity is 1. Figure 9 shows that the performance of Repart and Preagg+Repart stays the same when the Jaccard similarity changes. This means that repartition cannot utilize the similarities between datasets.

GRASP has better performance than LOOM for two reasons. First, GRASP is data distribution-aware and prioritize aggregation with more similarities. Second, GRASP has higher network utilization than LOOM. In GRASP, a fragment can be both sending and receiving as long as it is not working on the same partition. While in LOOM, a fragment is either a parent fragment receiving data or a child fragment sending data. We also evaluate with all-to-all aggregation. The result shows that GRASP has similar performance with repartition as there is no underutilization of network for all-to-all aggregation in this experiment and we omit the results.

### 5.2.2 Effect of similarity within fragments

In Section 5.2.1, there is only one tuple for each GROUP BY key within each fragment, hence local aggregation does not help in reducing the size of data, Preagg+Repart and Repart have the same performance. In this experiment, we evaluate how GRASP works when there are multiple tuples for one GROUP BY key within one fragment.

There are 128 million tuples in each fragment. We change the distinct cardinalities from 128 million, 64 million, 32 million to 16 million, which changes the number of tuples per GROUP BY key from 1, 2, 4, to 8. The smaller the

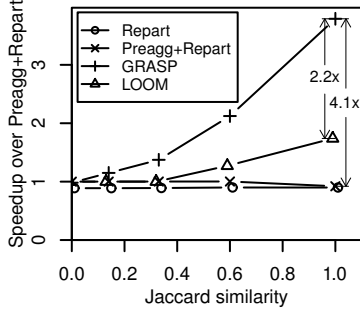


Figure 9: Speedup of GRASP when the similarity between datasets increases. GRASP is up to  $2.2\times$  faster than LOOM and  $4.1\times$  faster than Preagg+Repart.

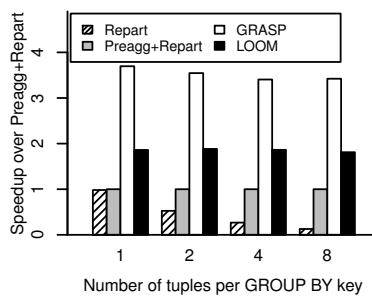


Figure 10: Speedup over Preagg+Repart when there are multiple tuples for each GROUP BY key in the same fragment for all-to-one aggregation.

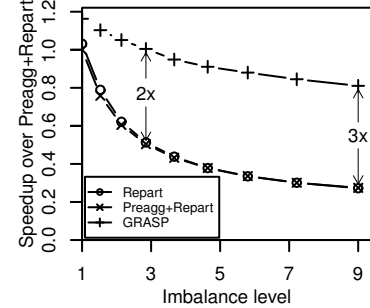


Figure 11: Speedup of GRASP for all-to-all aggregations when fragment 0 receives more tuples. GRASP is up to  $3\times$  faster than Preagg+Repart.

distinct cardinality is, the more tuples are aggregated by local aggregation.

The results for the all-to-one aggregation are shown in Figure 10. The horizontal axis is the number of tuples for each group by key within the same fragment. The vertical axis is speedup over Preagg+Repart. Higher bars means better performance. The results show that Preagg+Repart has better performance than Repart when the number of tuples for each group by key increase, which means more opportunities for local aggregation. However, GRASP always has better performance and is always more than  $3\times$  faster than Preagg+Repart and about  $2\times$  faster than than LOOM in all-to-one aggregations. GRASP has similar performance as Preagg+Repart in all-to-all aggregations as there is no underutilized network and we omit the result here. GRASP has the same or better performance than repartition and LOOM when the similarity within the same dataset changes.

### 5.2.3 Effect of workload imbalance

In parallel aggregation, some fragments may receive more tuples to aggregate for two reasons. First, the repartition function may assign more GROUP BY keys to some fragments. Second, even if each fragment gets the same number of GROUP BY keys to process, there may be skew in the dataset. In this section, we evaluate how GRASP works when one fragment gets more tuples to process.

In this experiment, we have 128 million tuples and  $R.a$  ranges from 1 to 128 million. We change the repartition function to assign more tuples to fragment 0. We assign  $n$  million tuples to fragment 0 for aggregation and assign  $m = \frac{128-n}{7}$  million tuples to the other fragments. We use  $l = \frac{n}{m}$  to denote the *imbalance level*. When  $n$  equals to 16,  $l$  is 1 and there is no imbalance. However, as  $n$  increases, fragment 0 gets more tuples than other fragments.

The results are shown in Figure 11. The horizontal axis is *imbalance level*  $l$ . The vertical axis is the speedup over Preagg+Repart when  $l$  is 0. Here speedup 1 corresponds to response time of 22.1 seconds. Notice that LOOM is not shown here because LOOM does not work for all-to-all aggregations. Figure 11 shows that the performance of repartition and GRASP both decreases when the workload imbalance increases. However, the performance decreases much faster for repartition than GRASP and GRASP is already  $2\times$  faster than Preagg+Repart when fragment 0 receives about 3 times of data of other fragments. This is

because in repartition, other fragments will stop receiving and aggregating data when they are waiting for fragment 0 to complete. While for GRASP, other fragments are still scheduled to receive and aggregate data. GRASP improves performance when some fragments process more tuples.

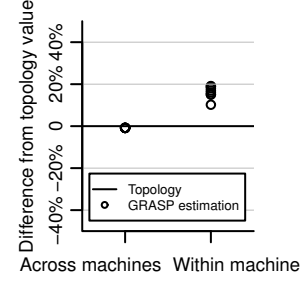


Figure 12: The comparison between the bandwidth from topology and estimated bandwidth from benchmarks.

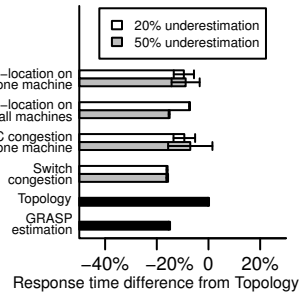


Figure 13: The speedup on the MODIS dataset when changing the estimated bandwidth.

## 5.3 Experiments with nonuniform bandwidth

The communication bandwidth between fragments can be nonuniform, i.e. different fragments communicate at different throughput, for two reasons. First, the network may be nonuniform. Fragments using different network links for communication can have different bandwidth. For data centers with high over-subscription ratio [17], machines within the same rack communicate with higher bandwidth than machines in different racks. Even HPC systems which strive for balanced networks can have nonuniform network too [20]. Second, the placement of fragments also leads to nonuniform bandwidth. For example, communication between fragments within the same machine have higher bandwidth than communication between fragments in different machine.

In this section, we show how GRASP works with nonuniform bandwidth between fragments by running multiple fragments in each machine.

### 5.3.1 Bandwidth approximation

The bandwidth estimation procedure described in Section 3.2 leads to two questions: how accurate is the estimation and how robust is GRASP to estimation errors?

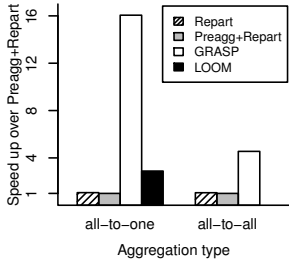


Figure 14: Speedup over Preagg+Repart with nonuniform bandwidth.

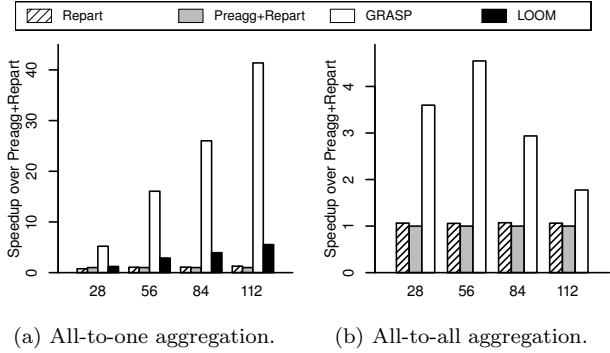
Figure 12 compares the available bandwidth as estimated by GRASP versus a manual calculation based on the hardware specifications, the network topology and the fragment placement. This experiment uses 8 machines with each machine having 14 fragments in the experiment. “Within machine” and “Across machines” corresponds to the communication bandwidth between fragments within the same node and across different nodes, respectively. The result shows that the estimation error is within 20% from the theoretical bandwidth. We conclude that the GRASP estimation procedure is fairly accurate in an idle cluster.

The estimation procedure may introduce errors in production clusters that are rarely idle. Figure 13 shows the impact of bandwidth underestimation on the response time of the aggregation plan produced by GRASP. We test two underestimation levels, 20% and 50% from the theoretical value. In this experiment we force GRASP to use a modified bandwidth matrix while running the aggregation query on the MODIS dataset. We run the experiment 10 times picking nodes at random for each setting, and show the standard deviation as the error bar. Co-location results in the underestimation of the communication bandwidth between local fragments in one or more machines. NIC contention and switch contention underestimates the available network bandwidth for one or all nodes in the cluster, respectively. “Topology” corresponds to the calculation based on the hardware capabilities, while “GRASP estimation” corresponds to the procedure described in Section 3.2. The horizontal axis is the response time difference with respect to the plan GRASP generated using the theoretical hardware capabilities (hence, lower means faster). The result shows that GRASP has better performance when using the estimated bandwidth matrix than the accurate bandwidth from network topology. This is because the estimated bandwidth measured from the benchmark is closer to the available bandwidth during query execution. Moreover, even when the available bandwidth is underestimated by up to 50%, the change in query response time is less than 20%. We conclude that GRASP is robust to errors introduced during bandwidth approximation.

### 5.3.2 Effect of nonuniform bandwidth

GRASP takes network bandwidth into consideration in aggregation scheduling. How well does GRASP work when the bandwidth of network links is different in the cluster?

In this experiment, we use 4 machines and each machine has 14 aggregation fragments. The dataset in each fragment has 14 million tuples with  $R.a$  ranging from 1 to 14 million. The result is shown in Figure 14. The vertical axis is the



(a) All-to-one aggregation. (b) All-to-all aggregation. Figure 15: Speedup over Preagg+Repart when scaling out.

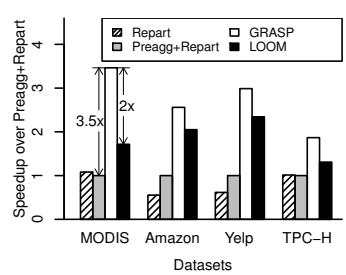


Figure 16: Speedup over Preagg+Repart on TPC-H workload and real datasets.

speedup over Preagg+Repart. The experiment results show that GRASP has better performance than both repartition and LOOM for both all-to-one and all-to-all aggregations. GRASP is up to 16× faster than Preagg+Repart and 5.6× faster than LOOM in all-to-one aggregation and 4.6× faster than Preagg+Repart in all-to-all aggregation. This is because GRASP is topology-aware and schedules more aggregations with faster network links. GRASP is topology-aware and has better performance with nonuniform bandwidth.

### 5.3.3 Effect of more plan fragments

GRASP considers the candidate aggregations between all plan fragments for all partitions in each phase of aggregation scheduling. Hence the cost of GRASP increases when there are more plan fragments. In this experiment, we evaluate how GRASP works when the number of fragments increases. We change the number of fragments from 28, 56, 84 to 112 by running 14 fragments per node and changing the number of nodes from 2, 4, 6 to 8. Each plan fragment has 16 million tuples with  $R.a$  ranging from 1 to 16 million.

The result is shown in Figure 15, where the horizontal axis is the number of fragments and the vertical axis is the speedup over Preagg+Repart. For all-to-one aggregations, Figure 15a shows that GRASP has better performance and is 41× faster than Preagg+Repart and 7.5× faster than LOOM when the number of fragments is 112. The speedup increases when the number of fragments increases. This is because in all-to-one aggregations, the receiving link of the final destination node is bottleneck for repartition. The performance of repartition degrades when the number of fragments increases. Another reason is that, the number of partitions from the “Partition & calculate minhash” step is constant when the number of fragments increases. Hence there are fewer candidate aggregations in each phase.

For all-to-all aggregations, Figure 15b shows that GRASP is 4.6× faster than Preagg+Repart when the number of fragments is 56. However, the speedup decreases for GRASP when the number of fragments exceeds 56 in all-to-all aggregations. This is because in all-to-all aggregations, all computing fragments get one or more partitions of data to process. The number of partitions is proportional to the number of fragments when the number of fragments increases. Hence the cost of GRASP is more expensive in all-to-all aggregations as there are more candidate aggregations.

### 5.3.4 Real datasets and TPC-H workload

These experiments evaluate the performance of the GRASP plans with the TPC-H workload and three real datasets. We

Repart	Preagg+Repart	LOOM	GRASP
3,464,926,620	3,195,388,849	2,138,236,114	787,105,152

Table 2: Tuples received by the final destination fragment.

use 8 machines and 14 fragments per machine. The dataset is aggregated to fragment 0, which corresponds to the all-to-one aggregation.

**Speedup results:** Figure 16 shows the speedup over Preagg+Repart for each algorithm. The result shows that GRASP has the best performance for all datasets. GRASP is 2× faster than LOOM and 3.5× faster than Preagg+Repart in the MODIS dataset.

**Network utilization:** Figure 17 shows the network utilization plot for the MODIS dataset. The horizontal axis is the time elapsed since the query was submitted to the coordinator. (Note that the scale of the horizontal axis is not the same, as some algorithms finish earlier than others.) Each horizontal line in the plot represents one incoming network link or one outgoing link of a fragment. For each link, we plot a line when there is traffic in the link and leave it blank otherwise.

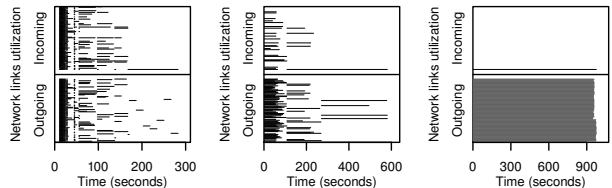
Figure 17a shows network utilization with GRASP. After a short delay to compute the aggregation plan, the network is fully utilized in the first few phases and there is traffic in all links. As the aggregation progresses, more fragments contain no data and hence these fragments do not further participate in the aggregation. The aggregation finishes in under 300 seconds.

Figure 17b shows LOOM. One can see that the network links, especially the receiving links, are not as fully utilized as in Figure 17a. The fan-in of the aggregation tree produced by LOOM is 5 for this experiment, which makes the receiving link of the parent fragment to be bottleneck. The aggregation finishes in about 600 seconds.

Figure 17c shows Preagg+Repart. All receiving links except fragment 0 (the aggregation destination) are not utilized. The entire aggregation is bottlenecked on the receiving capability of fragment 0. The aggregation takes more than 900 seconds. We omit the figure for Repart as it is similar to Preagg+Repart.

**Tuples transmitted to destination:** The GRASP performance gains can be directly attributed to the fact that it transmits less data on the incoming link of the destination fragment, which is frequently the bottleneck of the entire aggregation. Table 2 shows how many tuples the destination fragment receives under different algorithms. Local pre-aggregation has minimal impact as it is only effective when duplicate keys happen to be co-located on the same node. LOOM transmits fewer tuples to the destination fragment as tuples are combined in the aggregation tree before arriving at the final destination fragment. By aggressively combining fragments based on their similarity, GRASP transmits 2.7× less tuples than LOOM to the destination fragment.

**Accuracy of minhash estimation:** We also evaluate the accuracy of the minhash estimation with the MODIS dataset. Figure 18 shows the cumulative distribution function of the absolute error in estimating the size of the intersection between fragments when the cardinality of the input is accurately known. The result shows that the absolute error of the size of the intersection is less than 10% for 90% of the estimations. We conclude that the minhash estimation is ac-



(a) GRASP (b) LOOM (c) Preagg+repart  
Figure 17: Network link utilization.

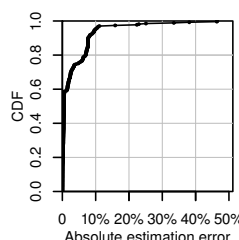


Figure 18: The error in minhash estimation.

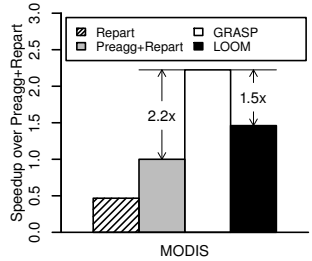


Figure 19: Speedup over Preagg+Repart on MODIS dataset in Amazon EC2.

curate and it allows GRASP to pick suitable fragment pairs for aggregation.

### 5.3.5 Evaluation on Amazon EC2

This section evaluates GRASP on the MODIS dataset on Amazon EC2. We allocate 8 instances of type d2.8xlarge and run 6 fragments in each instance. Figure 19 shows the speedup over the Preagg+Repart algorithm for each algorithm. Preagg+Repart has better performance than Repart in this experiment. This is because the fast 10 Gbps network in EC2 makes the query compute bound. The throughput of the local aggregation on pre-aggregated data is measured to be 811 MB/s, which is faster than aggregation on raw data with throughput to be 309 MB/s. This does not make difference in Section 5.3.4, as aggregation is network bound in the 1 Gbps network where the maximum throughput is 125 MB/s. However, the aggregation is compute bound in the 10 Gbps network of EC2 with a maximum throughput of 1.2 GB/s, hence pre-aggregation makes a big difference.

Figure 19 shows that GRASP is 2.2× faster than Preagg+Repart and 1.5× faster than LOOM. GRASP still has better performance when computation is the bottleneck. This is because GRASP maximizes network utilization by scheduling as many aggregations as possible in each phase, which also maximizes the number of fragments joining the aggregation and does the computation in each phase.

## 6. RELATED WORK

### Aggregation execution

Aggregation has been extensively studied in previous works. Some works focus on aggregation execution in a single server. Larson [24] studied how to use partial aggregation to reduce the input size of other operations. Cieslewicz and Ross [6] evaluated aggregation algorithms with independent and shared hash tables on multi-core processors. Ye et al. [53] compared different in-memory parallel aggregation algorithms on the Intel Nehalem architecture. Raman et al. [39] described the grouping and aggregation algorithm

used in DB2 BLU. Müller et al. [34] proposed an adaptive algorithm which combines the hashing and sorting implementations. Wang et al. [49] proposed a NUMA-aware aggregation algorithm. Jiang and Gagan [22] and Polychroniou et al [35] used SIMD and MIMD to parallelize the execution of aggregation. Gan et al. [13] optimized high cardinality aggregation queries with moment based summaries. Müller et al. [33] studied the floating-point aggregation in database systems.

Aggregation is also studied in parallel database systems. Graefe [15] introduced aggregation evaluation techniques in parallel database system. Shatdal and Naughton [46] proposed adaptive algorithms which switch between the re-partition and the two-phase algorithm at runtime. Aggregation trees are used in accelerating parallel aggregations. Melnik et al. [31] introduced Dremel, which uses a multi-level serving tree to execute aggregation queries. Yuan et al. [55] compared the interfaces and implementations for user-defined distributed aggregations in several distributed computing systems. Mai et al. [29] implemented NetAgg which aggregates data along network paths. Costa et al. [8] proposed Camdoop, which does in-network aggregation for a MapReduce-like system in a cluster with a direct-connect network topology. Yalagandula and Dahlin [52] designed a distributed information management system to do hierarchical aggregation in networked systems. Culhane et al. [9, 10] proposed LOOM, which builds an aggregation tree with fixed fan-in for all-to-one aggregations. LOOM first computes the ratio of the size of the final aggregation output to the size of the output of compute nodes. Here LOOM makes an implicit assumption that the size of the output of all compute nodes is the same. An optimal fan-in  $f$  is then calculated from the ratio and the number of compute nodes. An aggregation tree with the optimal fan-in  $f$  is generated, where each node in the aggregation tree takes input from  $f$  leaf nodes. One limitation of LOOM is that the size of aggregation outputs is unknown before aggregation execution. It is also unrealistic by implicitly assuming that all compute nodes have the same output size.

The impact of the network topology on aggregation has been studied. Gupta et al. [18] proposed an aggregation algorithm to deal with unreliable network such as sensor networks. Madden et al. [27] designed an acquisitional query processor for sensor networks to reduce power in query evaluation. Madden et al. [26, 28] also proposed a tiny aggregation service which does in network aggregation in sensor networks. Chowdhury et al. [5] proposed Orchestra to manage network activities in map reduce systems.

None of the above aggregation algorithms is aware of the similarity between datasets as GRASP does. The most relevant work is LOOM which considers the amount of data reduced in the aggregation. However LOOM only considers the overall reduction rate and fails to pick data with most similarities for aggregation.

#### *Dataset-aware algorithms*

Dataset-aware algorithms use information about the data distribution and data placement during query processing. Prior work has studied how to use data placement information to take advantage of locality. Some algorithms consider the offline setting. Zamanian et al. [56] introduced a data partitioning algorithm to maximize locality in the data distribution. Mozafari et al. [32] use the robust optimization theory in database design which is not only op-

timized for past workload, but also for uncertainties from future workloads. Prior research has also considered how to extract and exploit locality information at runtime. Rödiger et al. [43] proposed a locality-sensitive join algorithm which first builds a histogram for the workload, then schedules the join execution to reduce network traffic. Polychroniou [36] proposed track-join, where the distribution of the join key is exchanged across the cluster to generate a join schedule to maximally leverage locality. Lu et al. [25] proposed AdaptDB, which refines data partitioning according to the data access of queries at runtime.

Dataset-aware algorithms have also been proposed to deal with skewed datasets. DeWitt et al. [11] dealt with skew in join by first sampling the data, then partitioning the build relation and replicating the probe relation as needed. Shah et al. [45] implemented an adaptive partitioning operator to collect dataset information at runtime and address the problem of workload imbalance in continuous query systems. Xu et al. [51] addressed skew in parallel joins by first scanning the dataset to identify the skewed values, then keeping the skewed rows locally and duplicates the matching rows. Rödiger et al. [41] adopted similar approach as DeWitt et al. [11] by first sampling 1% of the data and then use this information to decide the data partition scheme. Wolf et al. [50] divided the parallel hash join into two phases, and add one scheduling phase to split the partition with data skew. Elseidy et al. [12] proposed a parallel online dataflow join which is resilient to data skew.

## 7. CONCLUSION AND FUTURE WORK

Parallel aggregation is a ubiquitous operation in data analytics. For low-cardinality parallel aggregations, the network cost involved is negligible when data is aggregated to a few tuples by local pre-aggregation. However, for high-cardinality aggregation, the network communication cost is significant. This paper proposes GRASP, an algorithm that schedules parallel aggregation in a distribution-aware manner to increase network utilization and reduce the communication cost for algebraic aggregations.

Looking ahead, GRASP can be further extended in two promising ways. First, GRASP can be extended for non-algebraic aggregations. This would require a new metric to quantify the data reduction of an aggregation pair. Second, the assumption that the communication cost dominates the aggregation marginally holds on 10Gbps networks, and will not hold in faster networks such as InfiniBand. The opportunity for GRASP is to augment the cost estimation formulas to account for compute overheads, instead of relying on the network transfer cost alone. This will jointly optimize computation and communication overheads during aggregation in high-performance networks.

## 8. REFERENCES

- [1] M. Al-Fares, A. Loukissas, and A. Vahdat. A scalable, commodity data center network architecture. *SIGCOMM Comput. Commun. Rev.*, 38(4):63–74, Aug. 2008.
- [2] P. Austrin, T. Pitassi, and Y. Wu. Inapproximability of treewidth, one-shot pebbling, and related layout problems. In *Approximation, Randomization, and Combinatorial Optimization. Algorithms and Techniques*, pages 13–24. Springer, 2012.

[3] A. Z. Broder, M. Charikar, A. M. Frieze, and M. Mitzenmacher. Min-wise independent permutations (extended abstract). In *Proceedings of the Thirtieth Annual ACM Symposium on Theory of Computing*, STOC '98, pages 327–336, New York, NY, USA, 1998. ACM.

[4] A. Cayley. A theorem on trees. *Quarterly Journal of Pure Applied Mathematics*, 23:376–378, 1889.

[5] M. Chowdhury, M. Zaharia, J. Ma, M. I. Jordan, and I. Stoica. Managing data transfers in computer clusters with orchestra. In *Proceedings of the ACM SIGCOMM 2011 Conference*, SIGCOMM '11, pages 98–109, New York, NY, USA, 2011. ACM.

[6] J. Cieslewicz and K. A. Ross. Adaptive aggregation on chip multiprocessors. In *Proceedings of the 33rd International Conference on Very Large Data Bases*, VLDB '07, pages 339–350. VLDB Endowment, 2007.

[7] <https://www.citusdata.com/blog/2018/03/09/distributed-execution-of-ctes-and-subqueries-in-citus/>.

[8] P. Costa, A. Donnelly, A. Rowstron, and G. O’Shea. Camdoop: Exploiting in-network aggregation for big data applications. In *Proceedings of the 9th USENIX Conference on Networked Systems Design and Implementation*, NSDI’12, pages 3–3, Berkeley, CA, USA, 2012. USENIX Association.

[9] W. Culhane, K. Kogan, C. Jayalath, and P. Eugster. Loom: Optimal aggregation overlays for in-memory big data processing. In *Proceedings of the 6th USENIX Conference on Hot Topics in Cloud Computing*, HotCloud’14, pages 13–13, Berkeley, CA, USA, 2014. USENIX Association.

[10] W. Culhane, K. Kogan, C. Jayalath, and P. Eugster. Optimal communication structures for big data aggregation. In *2015 IEEE Conference on Computer Communications, INFOCOM 2015, Kowloon, Hong Kong, April 26 - May 1, 2015*, pages 1643–1651, 2015.

[11] D. J. DeWitt, J. F. Naughton, D. A. Schneider, and S. Seshadri. Practical skew handling in parallel joins. In *Proceedings of the 18th International Conference on Very Large Data Bases*, VLDB ’92, pages 27–40, San Francisco, CA, USA, 1992. Morgan Kaufmann Publishers Inc.

[12] M. Elseidy, A. Elguindy, A. Vitorovic, and C. Koch. Scalable and adaptive online joins. *Proc. VLDB Endow.*, 7(6):441–452, Feb. 2014.

[13] E. Gan, J. Ding, K. S. Tai, V. Sharan, and P. Bailis. Moment-based quantile sketches for efficient high cardinality aggregation queries. *CoRR*, abs/1803.01969, 2018.

[14] A. Gionis, P. Indyk, and R. Motwani. Similarity search in high dimensions via hashing. In *Proceedings of the 25th International Conference on Very Large Data Bases*, VLDB ’99, pages 518–529, San Francisco, CA, USA, 1999. Morgan Kaufmann Publishers Inc.

[15] G. Graefe. Query evaluation techniques for large databases. *ACM Comput. Surv.*, 25(2):73–170, 1993.

[16] J. Gray, A. Bosworth, A. Layman, and H. Pirahesh. Data cube: A relational aggregation operator generalizing group-by, cross-tab, and sub-total. In *Proceedings of the Twelfth International Conference on Data Engineering*, February 26 - March 1, 1996, New Orleans, Louisiana, pages 152–159, 1996.

[17] A. G. Greenberg, J. R. Hamilton, N. Jain, S. Kandula, C. Kim, P. Lahiri, D. A. Maltz, P. Patel, and S. Sengupta. VL2: a scalable and flexible data center network. In *Proceedings of the ACM SIGCOMM 2009 Conference on Applications, Technologies, Architectures, and Protocols for Computer Communications*, Barcelona, Spain, August 16-21, 2009, pages 51–62, 2009.

[18] I. Gupta, R. v. Renesse, and K. P. Birman. Scalable fault-tolerant aggregation in large process groups. In *Proceedings of the 2001 International Conference on Dependable Systems and Networks (Formerly: FTCS)*, DSN ’01, pages 433–442, Washington, DC, USA, 2001. IEEE Computer Society.

[19] R. He and J. McAuley. Ups and downs: Modeling the visual evolution of fashion trends with one-class collaborative filtering. In *Proceedings of the 25th International Conference on World Wide Web*, WWW 2016, Montreal, Canada, April 11 - 15, 2016, pages 507–517, 2016.

[20] <https://htor.inf.ethz.ch/research/topologies/>.

[21] P. Indyk and R. Motwani. Approximate nearest neighbors: Towards removing the curse of dimensionality. In *Proceedings of the Thirtieth Annual ACM Symposium on Theory of Computing*, STOC ’98, pages 604–613, New York, NY, USA, 1998. ACM.

[22] P. Jiang and G. Agrawal. Efficient simd and mimd parallelization of hash-based aggregation by conflict mitigation. In *Proceedings of the International Conference on Supercomputing*, ICS ’17, pages 24:1–24:11, New York, NY, USA, 2017. ACM.

[23] S. Khot. On the power of unique 2-prover 1-round games. In *Proceedings of the thiry-fourth annual ACM symposium on Theory of computing*, pages 767–775. ACM, 2002.

[24] P. Larson. Data reduction by partial preaggregation. In *Proceedings of the 18th International Conference on Data Engineering*, San Jose, CA, USA, February 26 - March 1, 2002, pages 706–715, 2002.

[25] Y. Lu, A. Shanbhag, A. Jindal, and S. Madden. Adaptdb: Adaptive partitioning for distributed joins. *Proc. VLDB Endow.*, 10(5):589–600, Jan. 2017.

[26] S. Madden, M. J. Franklin, J. M. Hellerstein, and W. Hong. TAG: A tiny aggregation service for ad-hoc sensor networks. In *5th Symposium on Operating System Design and Implementation (OSDI 2002)*, Boston, Massachusetts, USA, December 9-11, 2002, 2002.

[27] S. Madden, M. J. Franklin, J. M. Hellerstein, and W. Hong. The design of an acquisitional query processor for sensor networks. In *Proceedings of the 2003 ACM SIGMOD International Conference on Management of Data*, SIGMOD ’03, pages 491–502, New York, NY, USA, 2003. ACM.

[28] S. Madden, R. Szewczyk, M. J. Franklin, and D. E. Culler. Supporting aggregate queries over ad-hoc wireless sensor networks. In *4th IEEE Workshop on Mobile Computing Systems and Applications (WMCSA 2002)*, 20-21 June 2002, Callicoon, NY, USA, pages 49–58, 2002.

[29] L. Mai, L. Rupprecht, A. Alim, P. Costa, M. Migliavacca, P. Pietzuch, and A. L. Wolf. Netagg:

Using middleboxes for application-specific on-path aggregation in data centres. In *Proceedings of the 10th ACM International on Conference on Emerging Networking Experiments and Technologies, CoNEXT '14*, pages 249–262, New York, NY, USA, 2014. ACM.

[30] S. Melnik, A. Gubarev, J. J. Long, G. Romer, S. Shivakumar, M. Tolton, and T. Vassilakis. Dremel: Interactive analysis of web-scale datasets. *PVLDB*, 3(1):330–339, 2010.

[31] S. Melnik, A. Gubarev, J. J. Long, G. Romer, S. Shivakumar, M. Tolton, and T. Vassilakis. Dremel: Interactive analysis of web-scale datasets. *PVLDB*, 3(1):330–339, 2010.

[32] B. Mozafari, E. Z. Y. Goh, and D. Y. Yoon. Cliffguard: A principled framework for finding robust database designs. In *Proceedings of the 2015 ACM SIGMOD International Conference on Management of Data, SIGMOD '15*, pages 1167–1182, New York, NY, USA, 2015. ACM.

[33] I. Müller, A. Arteaga, T. Hoefer, and G. Alonso. Reproducible floating-point aggregation in rdbmss. *CoRR*, abs/1802.09883, 2018.

[34] I. Müller, P. Sanders, A. Lacurie, W. Lehner, and F. Färber. Cache-efficient aggregation: Hashing is sorting. In *Proceedings of the 2015 ACM SIGMOD International Conference on Management of Data, SIGMOD '15*, pages 1123–1136, New York, NY, USA, 2015. ACM.

[35] O. Polychroniou, A. Raghavan, and K. A. Ross. Rethinking SIMD vectorization for in-memory databases. In *Proceedings of the 2015 ACM SIGMOD International Conference on Management of Data, SIGMOD '15*, pages 1493–1508, New York, NY, USA, 2015. ACM.

[36] O. Polychroniou, R. Sen, and K. A. Ross. Track join: Distributed joins with minimal network traffic. In *Proceedings of the 2014 ACM SIGMOD International Conference on Management of Data, SIGMOD '14*, pages 1483–1494, New York, NY, USA, 2014. ACM.

[37] P. Raghavendra and D. Steurer. Graph expansion and the unique games conjecture. In *Proceedings of the forty-second ACM symposium on Theory of computing*, pages 755–764. ACM, 2010.

[38] P. Raghavendra, D. Steurer, and M. Tulsiani. Reductions between expansion problems. In *Computational Complexity (CCC), 2012 IEEE 27th Annual Conference on*, pages 64–73. IEEE, 2012.

[39] V. Raman, G. Attaluri, R. Barber, N. Chainani, D. Kalmuk, V. KulandaiSamy, J. Leenstra, S. Lightstone, S. Liu, G. M. Lohman, T. Malkemus, R. Mueller, I. Pandis, B. Schiefer, D. Sharpe, R. Sidle, A. Storm, and L. Zhang. Db2 with blu acceleration: So much more than just a column store. *Proc. VLDB Endow.*, 6(11):1080–1091, Aug. 2013.

[40] [https://docs.aws.amazon.com/redshift/latest/dg/c\\_high\\_level\\_system\\_architecture.html](https://docs.aws.amazon.com/redshift/latest/dg/c_high_level_system_architecture.html).

[41] W. Rödiger, S. Idicula, A. Kemper, and T. Neumann. Flow-join: Adaptive skew handling for distributed joins over high-speed networks. In *32nd IEEE International Conference on Data Engineering, ICDE 2016, Helsinki, Finland, May 16-20, 2016*, pages 1194–1205, 2016.

[42] W. Rödiger, T. Mühlbauer, A. Kemper, and T. Neumann. High-speed query processing over high-speed networks. *PVLDB*, 9(4):228–239, 2015.

[43] W. Rödiger, T. Mühlbauer, P. Unterbrunner, A. Reiser, A. Kemper, and T. Neumann. Locality-sensitive operators for parallel main-memory database clusters. In *IEEE 30th International Conference on Data Engineering, Chicago, ICDE 2014, IL, USA, March 31 - April 4, 2014*, pages 592–603, 2014.

[44] V. Satuluri and S. Parthasarathy. Bayesian locality sensitive hashing for fast similarity search. *Proc. VLDB Endow.*, 5(5):430–441, Jan. 2012.

[45] M. A. Shah, J. M. Hellerstein, S. Chandrasekaran, and M. J. Franklin. Flux: An adaptive partitioning operator for continuous query systems. In *Proceedings of the 19th International Conference on Data Engineering, March 5-8, 2003, Bangalore, India*, pages 25–36, 2003.

[46] A. Shatdal and J. F. Naughton. Adaptive parallel aggregation algorithms. In *Proceedings of the 1995 ACM SIGMOD International Conference on Management of Data, SIGMOD '95*, pages 104–114, New York, NY, USA, 1995. ACM.

[47] E. Vermote-NASA GSFC and MODAPS SIPS - NASA. (2015). MOD09 MODIS/Terra L2 Surface Reflectance, 5-Min Swath 250m, 500m, and 1km. NASA LP DAAC.

[48] E. Vermote-NASA GSFC and MODAPS SIPS - NASA. (2015). MOD09A1 MODIS/Surface Reflectance 8-Day L3 Global 500m SIN Grid. NASA LP DAAC.

[49] L. Wang, M. Zhou, Z. Zhang, M. Shan, and A. Zhou. Numa-aware scalable and efficient in-memory aggregation on large domains. *IEEE Trans. Knowl. Data Eng.*, 27(4):1071–1084, 2015.

[50] J. L. Wolf, P. S. Yu, J. Turek, and D. M. Dias. A parallel hash join algorithm for managing data skew. *IEEE Trans. Parallel Distrib. Syst.*, 4(12):1355–1371, Dec. 1993.

[51] Y. Xu, P. Kostamaa, X. Zhou, and L. Chen. Handling data skew in parallel joins in shared-nothing systems. In *Proceedings of the 2008 ACM SIGMOD International Conference on Management of Data, SIGMOD '08*, pages 1043–1052, New York, NY, USA, 2008. ACM.

[52] P. Yalagandula and M. Dahlin. A scalable distributed information management system. In *Proceedings of the 2004 Conference on Applications, Technologies, Architectures, and Protocols for Computer Communications, SIGCOMM '04*, pages 379–390, New York, NY, USA, 2004. ACM.

[53] Y. Ye, K. A. Ross, and N. Vesdapunt. Scalable aggregation on multicore processors. In *Proceedings of the Seventh International Workshop on Data Management on New Hardware, DaMoN '11*, pages 1–9, New York, NY, USA, 2011. ACM.

[54] <https://www.yelp.com/dataset/documentation/json>.

[55] Y. Yu, P. K. Gunda, and M. Isard. Distributed aggregation for data-parallel computing: Interfaces and implementations. In *Proceedings of the ACM SIGOPS 22Nd Symposium on Operating Systems*

*Principles*, SOSP '09, pages 247–260, New York, NY, USA, 2009. ACM.

[56] E. Zamanian, C. Binnig, and A. Salama. Locality-aware partitioning in parallel database systems. In *Proceedings of the 2015 ACM SIGMOD International Conference on Management of Data*, SIGMOD '15, pages 17–30, New York, NY, USA, 2015. ACM.